Theoretical Prediction of the Soil Thermal Conductivity at Moderately High Temperatures

Fabio Gori
e-mail: gori@uniroma2.it

Sandra Corasaniti

Department of Mechanical Engineering,
University of Rome "Tor Vergata",
Via di Tor Vergata, 110,
Rome, 00133, Italy

The theoretical model of the present paper assumes the unit cell of the porous medium as composed of a cubic space with a cubic solid particle at the center. The thermal conductivity is evaluated by solving the heat conduction equation with the assumption of parallel isotherms within the cubic space. The liquid water in the porous medium is distributed around the solid particle according to the phenomena of adsorption and capillarity. The thermal conductivity of the gas present within the pores takes into account the thermal conductivity of the water vapor and dry air, without enhanced vapor diffusion. The model simplifies the variation of the relative humidity, from dryness to the field capacity, with a linear increase. The predicted results, compared to experimental data, show the agreement is very good at the temperatures in the range (30–50°C) and acceptable at 70°C. At high temperature (90°C) the predictions are higher than the experiments and a better agreement could be obtained by decreasing the thermal conductivity of the gas phase. Besides, the trend of the theoretical predictions is in good agreement with the experiments also at high temperatures. [DOI: 10.1115/1.1513573]

Keywords: Conduction, Heat Transfer, Modeling, Porous Media, Thermophysical

Introduction

The prediction of the effective thermal conductivity of soils is very important in many heat and mass transfer phenomena related to ground, including waste disposal in unsaturated geologic media, geothermal energy extraction, drying problems in multiphase heat and mass transfer in porous and fractured media, enhanced oil recovery, radioactive waste storage, ground heat pumps and heat exchangers, forest fires and related problems, heat transfer from high voltage power cables, thermal soil remediation and soil behavior under forest fires. The effective thermal conductivity is dependent on a wide variety of properties related to the soil, including mineral composition of the solid particles, dry density, porosity, temperature and water content.

A soil is a multiphase porous medium. A dry or water saturated soil is a two-phases medium, composed of solid particle and gas or liquid water, respectively. A soil partially saturated by water is a three-phases medium, with the liquid water disposed among the solid particle by adsorption and capillarity [1]. In a partially saturated soil, heat and mass transfer are coupled by several mechanisms of thermally induced and water potential-induced flow of water in liquid and vapor phases [2]. If the temperature is below the freezing point, part of the water can be in the solid state and, according to the conditions in the porous medium, liquid water can coexist, as unfrozen water, with the solid ice to form a four-phases medium. Besides the large spectrum of problems identified, the interest of the present paper is focused on three-phases soils at temperatures in the range 30–90°C. Several experimental measurements are present in the literature at high temperatures [3–7]. The soils measured span many different types, varying in mineral composition, dry density, porosity and water content. Because of the large variety of experiments, the present paper focuses on the results of [3], in order to show the general agreement and the trend of the theoretical predictions.

A review of the literature has revealed that many theoretical and experimental studies have been carried out to determine the effective thermal conductivity of porous media. In the past years some experimental results measured the thermal conductivity of saturated and two-phases porous media. Theoretical models have been proposed, but the studies on the thermal conductivity of unsaturated porous media are limited.

Two recent papers [8,9] compared some modeling approaches to predict the effective thermal conductivity of high temperature soils. Two of the models tested in [8] are modifications of the original one of de Vries [4]. The third theoretical model was originally proposed in [10] for four-phases soils in partially frozen conditions and later modified for bricks [11]. A model for the thermal conductivity of unconsolidated porous medium, based on capillary pressure-saturation relation, has been proposed in [12]. A relation was obtained for the thermal conductivity of the unsaturated porous medium when $K_w/K_s \leqslant 0.2$. The stagnant thermal conductivity of spatially periodic porous media has been studied in [13]. Two models to predict the effective thermal conductivity of consolidated porous media, like cellular ceramics, have been developed in [14]. A model to determine the thermal conductivity of a bed of solid spherical particles, immersed in a static fluid, when the conductivity of the matrix solid is greater than that of the gas, has been formulated in [15].

The present paper presents a further enhancement of the model proposed in [10], with modifications that take into account the specific nature of the soil investigated, including the Permanent Wilting Point and the Field Capacity. Permanent Wilting Point is defined as the water remaining in the soil in the smallest of the micropores and around individual soil particles. Field Capacity is the water content present in the soil after a day, when rain has stopped and the irrigation water has been shut off. At this time the examination of the soil will show water has moved out of the macropores, its place has been taken by air, but the small pores remain filled with water.

Theoretical Approach

The present model is based on the assumption that the unit cell of the soil is composed of a cubic space with a cubic solid particle at the center. Figure 1 presents the cubic cell in the case of a two-phases medium where the continuous phase can be air (dry soil) or water (fully saturated soil). The main physical assumption of the cubic cell, no contact among adjoining particles, is the

Contributed by the Heat Transfer Division for publication in the JOURNAL OF HEAT TRANSFER. Manuscript received by the Heat Transfer Division July 20, 2001; revision received May 17, 2002. Associate Editor: C. T. Avedisian.

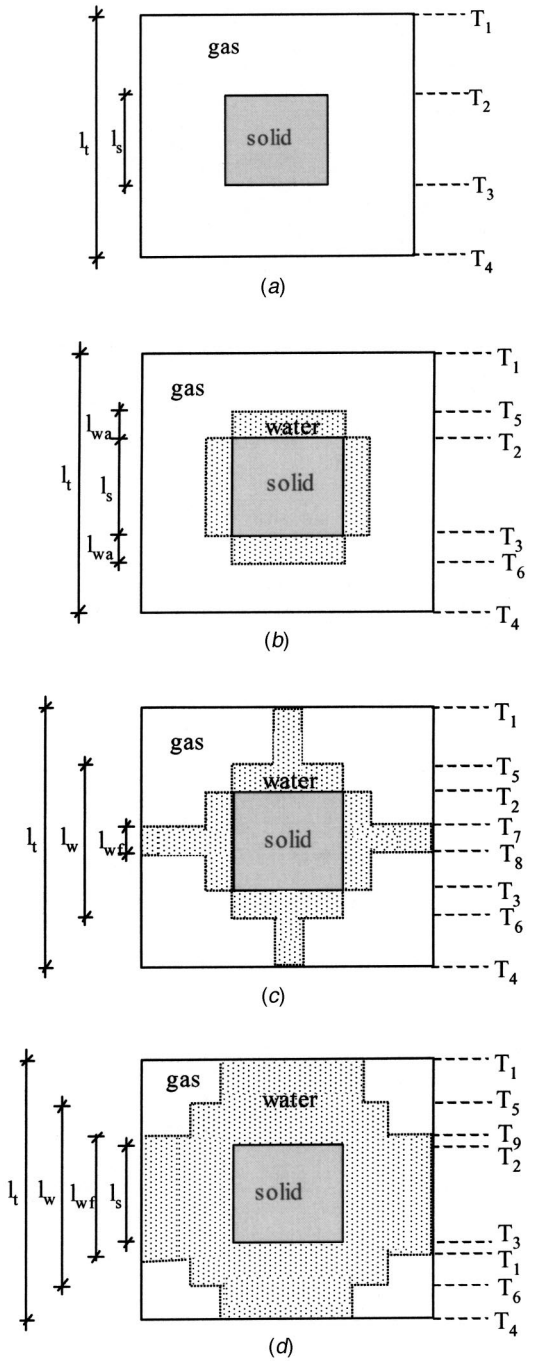

Fig. 1 (*a*) Cubic cell for two-phases dry soil; (*b*) cubic cell for three-phases soil at low water content; (*c*) cubic cell for three-phases soil in unsaturated conditions; and (*d*) cubic cell for three-phases soil near saturation conditions

answer to spherical particles with a point of contact, which is a negligible cross section for heat transfer. When water is present the major contribution to heat conduction is given by the cross section of the water bridge formed between the two particles. The porosity of the soil, ε, is taken into account by the ratio of the void volume to the total volume of the cell. The dimensions of the cubic cell, although reported in Fig. 1, do not need to be considered, because they can be expressed as ratios with the solid particle as in the following. The ratio of the lengths of the cubic cell and of the solid particle, as reported in Fig. 1, is:

$$\beta = \frac{l_t}{l_s} = \sqrt[3]{\frac{\rho_s}{\rho_d}} = \sqrt[3]{\frac{1}{1-\varepsilon}} \tag{1}$$

where ρ_s is the solid particles density and ρ_d the dry density of the soil.

The effective thermal conductivity of the unit cell can be evaluated by solving the heat conduction equation, with the assumptions of parallel isotherms or parallel heat flux lines. The parallel isotherms assumption, adopted in [10–11], is based on the hypothesis of a very high thermal conductivity in the transverse direction, while the parallel heat flux lines is valid when the thermal conductivity, in the transverse direction, is zero. Both assumptions have been tested in [16] for two-phases media.

The effective thermal conductivity of the medium has been evaluated in the present paper with the parallel isotherm hypothesis and is called K_T. For the two-phases porous medium of Fig. 1(*a*), K_T is given by:

$$\frac{1}{K_T} = \frac{\beta - 1}{K_c \cdot \beta} + \frac{\beta}{K_c \cdot (\beta^2 - 1) + K_s} \tag{2}$$

where K_c is the thermal conductivity of the gas (air and water vapor in general but water if fully saturated), and K_s the thermal conductivity of the solid particle. The first term in Eq. (2) corresponds to the thermal resistance of the gas in the cross section (l_t^2) and length $(l_t - l_s)$, while the second term is the thermal resistance of the materials gas-solid in the cross section (l_t^2) and length (l_s).

When the soil is neither dry nor fully saturated by water, water is distributed inside the cubic cell according to adsorption and capillarity. If the water content is very low, water is adsorbed around the solid particle, as assumed in Fig. 1(*b*). The adsorbed water W_c, is assumed empirically to be a fraction of the water content at the permanent wilting point W_P, according to [17], as

$$W_C = c W_P \tag{3}$$

where the constant c depends on the type of soils investigated. The present paper assumes $c \approx 0.375$ as suggested in [18]. The adsorbed water W_c, as given by Eq. (3), is the only empirical assumption of the present model.

When the water content, W, is greater than W_c, water bridges are establishes among the six solid particles surrounding the cubic cell, with the distributions assumed in Fig. 1(*c*) or 1(*d*), depending on the amount of water content. The effective thermal conductivity of the unit cell can be evaluated, with the assumption of parallel isotherms, and the expressions are reported in Appendix A.

Comparisons With Experimental Results

The soils investigated in [3] are reported in Table 1 below. The soils of Table 1 belong to three textural groups of soils: coarse, medium-fine and fine, as reported in the first column. The name of the soil is in the second column. The third column presents the range of dry density measured. The quartz content percentage is in the fourth column. The thermal conductivity of the solid particles of each soil, according to the evaluation carried out in [3], is reported in the fifth column. Volkmar soil has a thermal conductivity more than two times higher than the other soils because its quartz content is 97 percent. In the other soils the quartz content vary from 35 percent for Palouse B to 55 percent for Mokins. The sixth column shows the porosity range, corresponding to the dry densities of the third column, as evaluated in [3]. The last two columns show the Permanent Wilting Point water content W_P, and the Field Capacity W_F, as evaluated in [8]. The experimental data of [3] were found with the transient thermal probe method.

The thermal conductivity of water is assumed a function of the temperature T_C, (in °C), according to:

$$K_w = 0.569 + 1.88\ \ 10^{-3}\ \ T_C - 7.72\ \ 10^{-7}\ \ T_C^2 \tag{4}$$

Table 1 Experimental data [3]

Textural Group	Soil	ρ_d (g/cm^3)	% Quartz	K_s (W/m K)	ε	W_P (%)	W_F (%)
Coarse	L-soil	1.15 – 1.7	38	2.61	0.4 – 0.59	5.2	9.9
Coarse	Volkmar	1.27 – 1.69	97	4.71	0.362 – 0.52	8.6	15.7
Coarse	Royal	1.09 – 1.51	42.5	2.57	0.432 – 0.59	9.9	20.3
Medium - fine	Walla-Walla	0.94 – 1.52	48.4	2.53	0.429 – 0.647	9.6	26.2
Medium – fine	Palouse A	1.11 – 1.52	38.5	2.31	0.425 – 0.58	12.9	30.9
Medium – fine	Salkum	0.99 – 1.31	45.5	2.21	0.508 – 0.628	13.9	30.0
Medium - fine	Mokins	0.94 – 1.47	55	2.64	0.45 – 0.648	15.1	30.8
Fine	Palouse B	0.86 – 1.38	35	2	0.482 – 0.677	26	40.7

The thermal conductivity of air, equal to $K_a = 0.026$ W/m K at 27°C, is assumed variable with the temperature T_C, (in °C), according to the following equation:

$$K_a = 0.02408 + 0.0000792 \cdot T_C \tag{5}$$

In a partially saturated soil the thermal conductivity of the gas, present in the pore space, is due to water vapor mixed to air. The apparent thermal conductivity of the mixture of air and water vapor is then given by:

$$K_{\text{app}} = K_a + \phi \cdot K_{vs} \cdot \xi \tag{6}$$

where ϕ is the relative humidity of the gas mixture and ξ is the mass transfer enhancement factor, assumed by some investigations as $\xi > 1$, because of the phenomenon of enhanced vapor-phase diffusion. The thermal conductivity of water vapor is [8]:

$$K_{vs} = \frac{H_L \cdot D}{R_v \cdot T} \cdot \frac{p_b}{p_b - p_{vs}} \cdot \frac{dp_{vs}}{dT}; \tag{7}$$

where

$$R_v = \frac{R}{M_w}; \tag{8}$$

$$H_L = 2503 - 2.3 \cdot T_C; \tag{9}$$

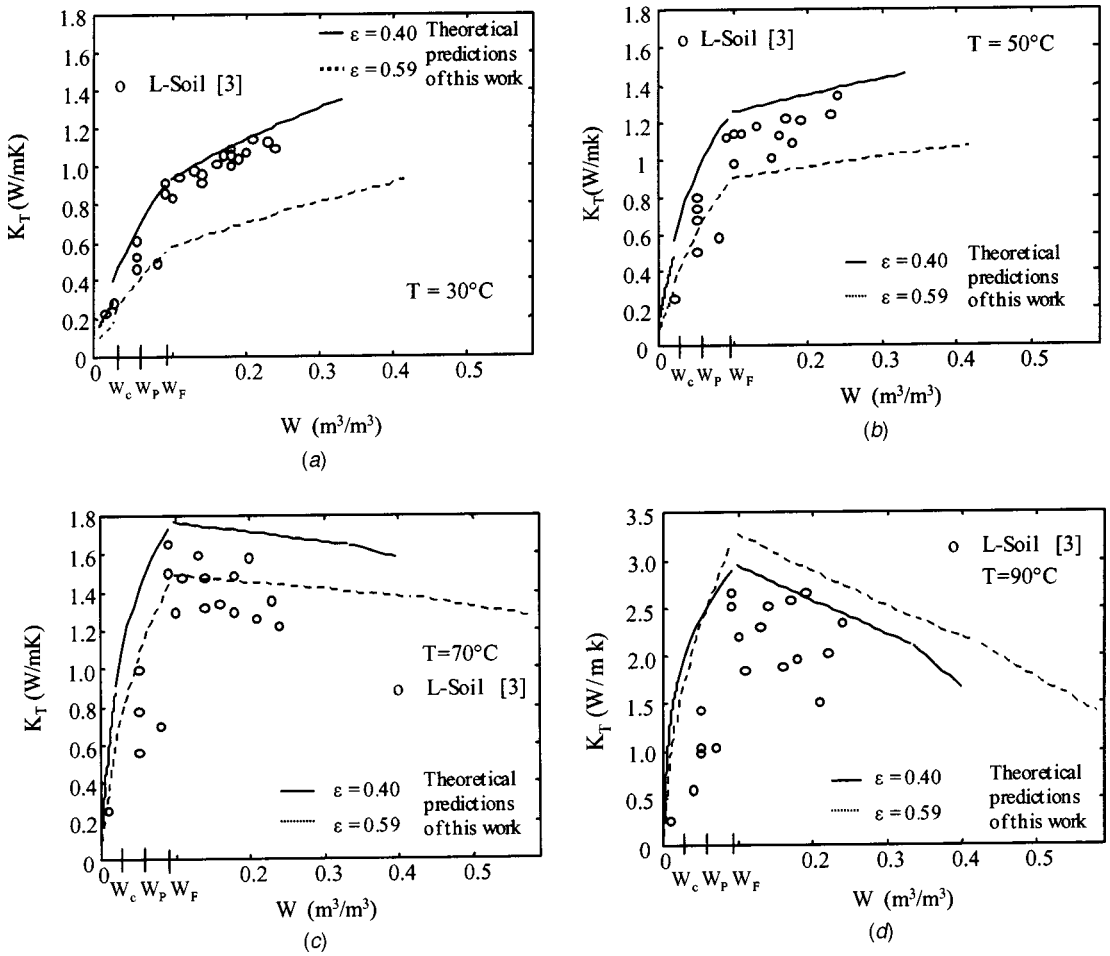

Fig. 2 (*a*) Effective thermal conductivity versus water content in *L*-soil [3]; (*b*) effective thermal conductivity versus water content in *L*-soil [3]; (*c*) Effective thermal conductivity versus water content in *L*-soil [3]; and (*d*) effective thermal conductivity versus water content in *L*-soil [3]

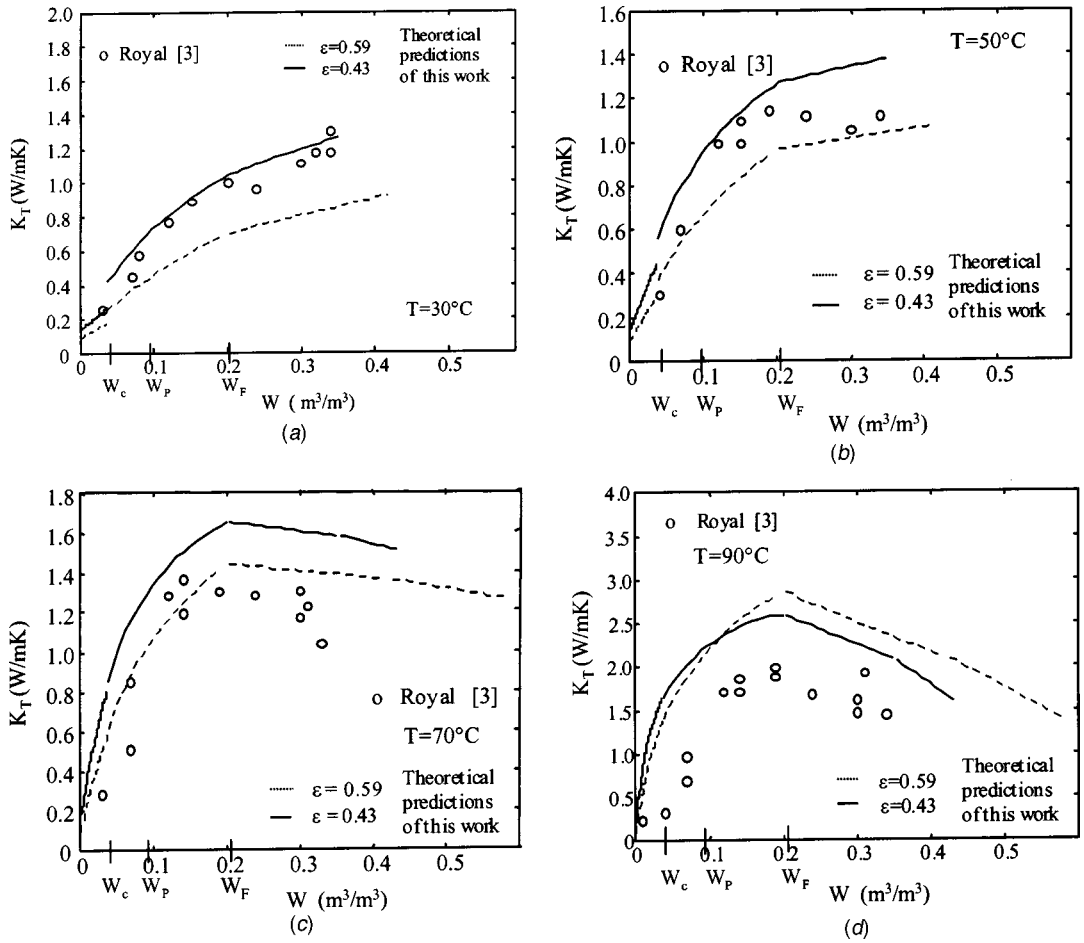

Fig. 3 (*a*) **Effective thermal conductivity versus water content in Royal soil [3]; (*b*) effective thermal conductivity versus water content in Royal soil [3]; (*c*) Effective thermal conductivity versus water content in Royal soil [3]; and (*d*) Effective thermal conductivity versus water content in Royal soil [3]**

$$D = 2.25 \cdot 10^{-5} \left[\frac{T}{273.15} \right]^{1.72}. \tag{10}$$

In the present model, on the basis of the discussion carried on in [19], the mass transfer enhancement factor ξ is assumed 1.

The Field Capacity of a soil is the condition when water has drained out of the larger pores but the small pores remain filled with water. In this situation, the air, trapped among the water bridges, contains water saturated vapor, i.e., the relative humidity, ϕ, of the gas space is equal to 1. On the other hand, $\phi = 0$ only in perfect dry conditions; i.e., with water content equal to zero. This is in agreement with [2] where the relative humidity is a function of the soil water content, according to an *s*-shaped curve, variable from zero, at zero water content, up to 100 percent, at a water content which depends on the type of soil. In order to simplify the present theoretical model, this work assumes the relative humidity as linearly variable from zero, at full dryness, to 100 percent, at the Field Capacity water content.

In summary, the thermal conductivity of the gas phase (air and water vapor) is given by Eq. (6), with $\xi = 1$, and the relative humidity is linearly variable with the water content, from dryness to field capacity, as

$$\phi = W / W_F \tag{11}$$

The linear variation is only a hypothesis which can be removed with the more correct assumption of a *s*-shaped curve, but, in a simple theoretical model like this, and with several complicated theoretical relations it seems very plausible.

Substituting the numerical values of Eq. (7–10) in Eq. (6), the apparent thermal conductivity is given by

$$K_{\text{app}} = K_a + 0.120 \cdot \phi; \quad \text{at } 30°C, \tag{12}$$

$$K_{\text{app}} = K_a + 0.335 \cdot \phi; \quad \text{at } 50°C, \tag{13}$$

$$K_{\text{app}} = K_a + 0.962 \cdot \phi; \quad \text{at } 70°C, \tag{14}$$

$$K_{\text{app}} = K_a + 4.474 \cdot \phi; \quad \text{at } 90°C, \tag{15}$$

where the thermal conductivity of dry air is variable with the temperature according to the Eq. (5). Above the Field Capacity water content, W_F, the apparent thermal conductivity of the gas is given by

$$K_{\text{app}} = K_a + K_{vs} \tag{16}$$

Figures 2–6 present the theoretical predictions of this work. Each prediction can be subdivided in four regions. The first region, extending from zero water content to W_C, given by Eq. (3), corresponds to the condition of water adsorbed around the solid particle (Fig. 1(*b*)) and it gives the lowest thermal conductivity because of the absence of water bridges between the adjoining solid particles. The first discontinuity between the first and the second region is due to the appearance of water bridges. In the second region, from W_C to W_F, water bridges are present among

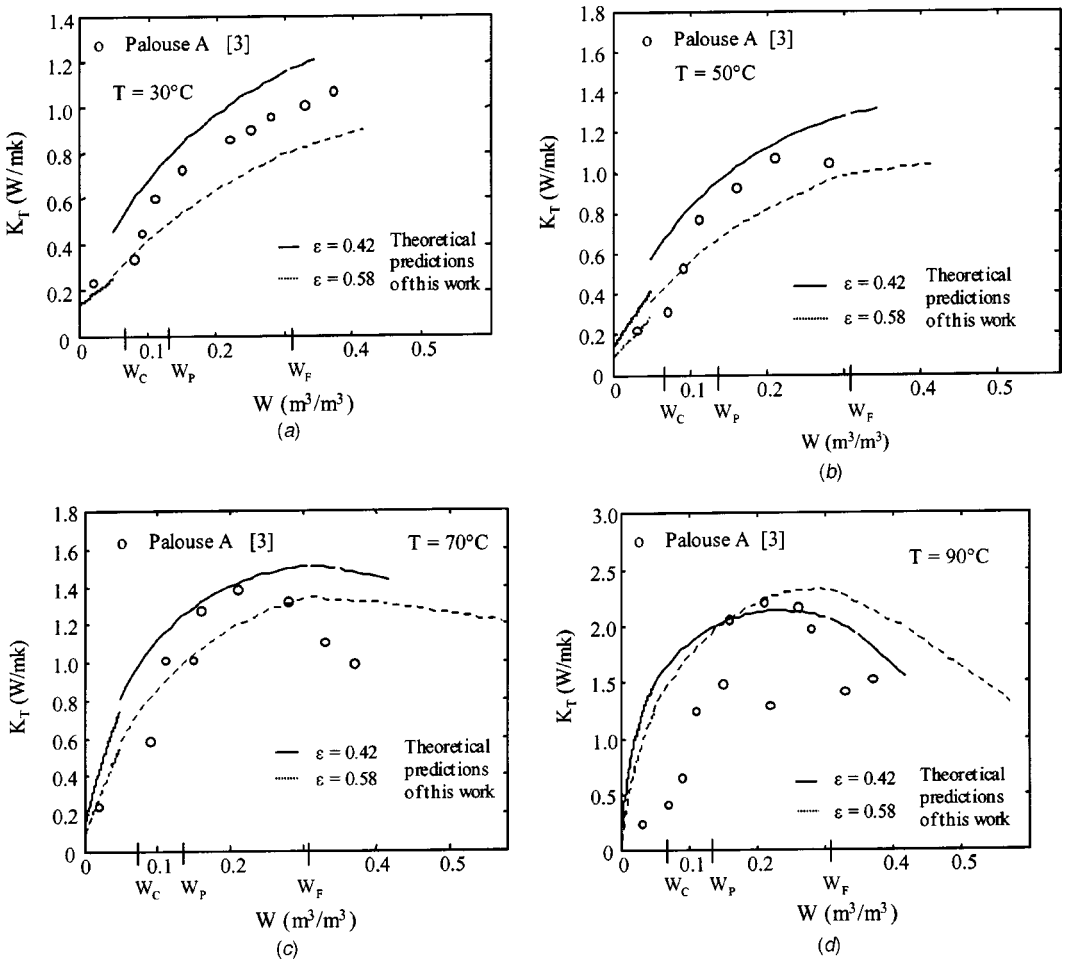

Fig. 4 (*a*) Effective thermal conductivity versus water content in Palouse A [3]; (*b*) effective thermal conductivity versus water content in Palouse A [3]; (*c*) effective thermal conductivity versus water content in Palouse A [3]; and (*d*) effective thermal conductivity versus water content in Palouse A [3]

the solid particles, due to capillarity (Fig. 1(*c*)). A continuous increase of K_T, up to the Field Capacity of the soil, W_F, is predicted because of the variation of the relative humidity, as given by Eq. (11). A second discontinuity in the model is present at the Field Capacity, W_F. The third region starts at W_F extending up to the third discontinuity, which is due to the transition from the water configuration of Fig. 1(*c*) to that of Fig. 1(*d*) and is specific of the present theoretical model. The fourth region starts at the third discontinuity and extends up to saturation. In the third and fourth regions, at the two highest temperatures (70°C and 90°C), the effective thermal conductivity decreases for $W > W_F$, because the thermal conductivity of water (at saturation) is lower than the apparent thermal conductivity given by Eq. (6).

Figures 2–3 compare the theoretical predictions of this work with the experimental measurements of two of the coarse soils of Table 1 [3]. Figure 2 shows the data for *L*-Soil, which has the smallest quartz content (38 percent), Wilting Point (5.2 percent) and Field Capacity (9.9 percent). Two theoretical predictions are reported in each figure for two porosities, which correspond to the extremes values of the dry densities of Table 1. The two predictions are in fair agreement with the experiments at 30°C (Fig. 2(*a*)) and 50°C (Fig. 2(*b*)), in the whole range of water content. The predictions are a little higher than the experiments at 70°C (Fig. 2(*c*)) and higher at 90°C (Fig. 2(*d*)). Note that the change in the slope of the predictions at the Field Capacity is in good agreement with the slope change of the experimental data [3].

Figure 3 presents the predictions and the data for Royal soil, which has a moderate quartz content (42.5 percent) and Field Capacity (20.3 percent). The predictions are in good agreement to the experiments at 30°C (Fig. 3(*a*)) and 50°C (Fig. 3(*b*)), in the complete range of water content. Indeed, the data are within the predictions obtained with the two porosities reported in Table 1 [3]. At 70°C (Fig. 3(*c*)) the predictions are in good agreement below the field capacity but somewhat higher than the experiments at higher water contents. At 90°C (Fig. 3(*d*)) the theoretical predictions are higher than the experiments in the whole range of water content. Also for Royal soil it is evident that the slope change, in the experimental as well as in the theoretical results, occurs around the field capacity (20.3 percent). Further on, at the field capacity the soil exhibits the highest thermal conductivity, for the temperatures of 70°C and 90°C.

Figures 4–5 present the theoretical predictions compared to the experimental data of two medium-fine soils of Table 1; i.e., Palouse A and Salkum. The conclusions are similar to those made with Figs. 1–2. The agreement is fairly good at the temperatures 30°C and 50°C (Figs. 4(*a*,*b*) and 5(*a*,*b*). It is acceptable at 70°C up to the Field Capacity (Fig. 4(*c*) and Fig. 5(*c*)). The predictions are higher than the experiments at 90°C (Figs. 4(*d*) and 5(*d*).

Finally Fig. 6 presents the predictions and the experiments of the only fine soil of Table 1; i.e., Palouse B. Figure 6(*a*,*b*) present a fairly good agreement. Figure 6(*c*,*d*) show the model provides higher values than the experiments with conclusions similar to the previous ones.

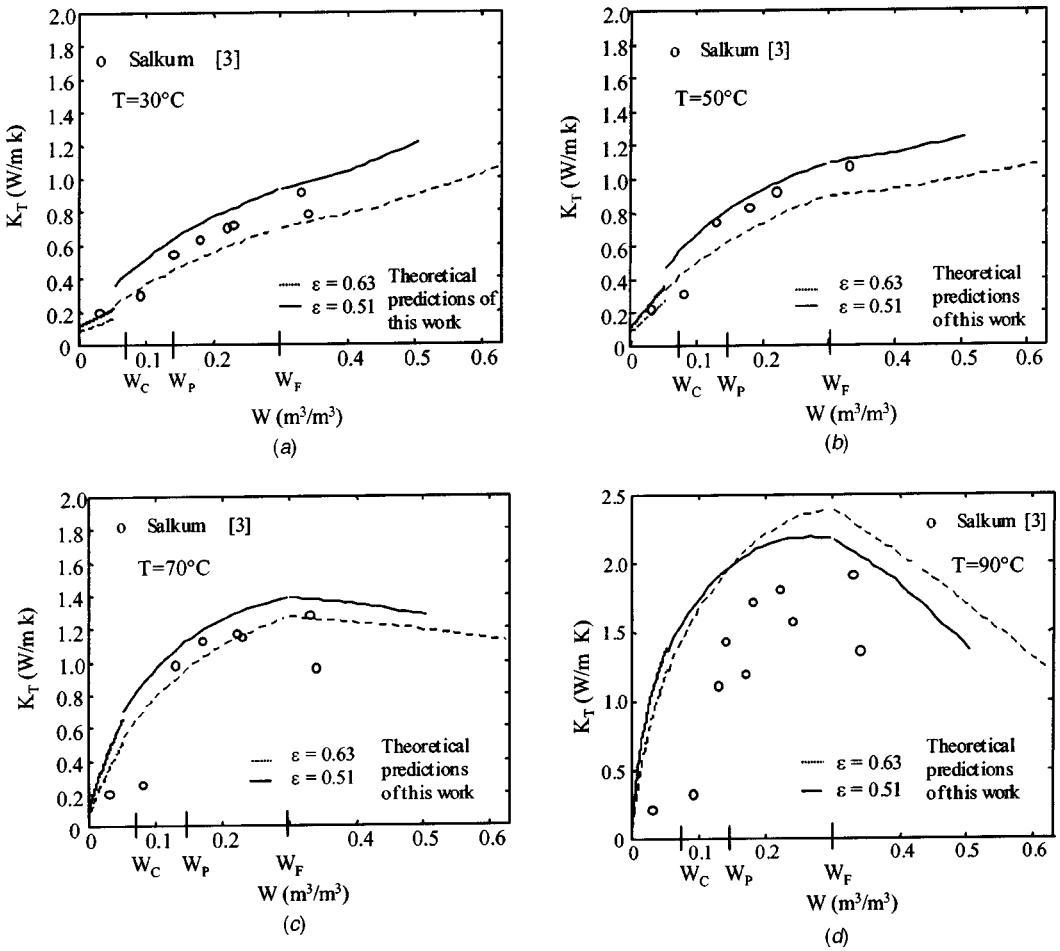

Fig. 5 (*a*) **Effective thermal conductivity versus water content in Salkum [3];** (*b*) **effective thermal conductivity versus water content in Salkum [3];** (*c*) **effective thermal conductivity versus water content in Salkum [3]; and** (*d*) **effective thermal conductivity versus water content in Salkum [3]**

Conclusions

The theoretical model, used to simulate three-phases porous soils, gives predictions in very good agreement with the experimental results at the temperatures of 30°C and 50°C. At the temperature of 70°C the agreement is fairly good from dryness to the Field Capacity. The predictions are somewhat higher than the experiments, above the field capacity. At 90°C the predictions are higher than the experiments almost everywhere and a better comparison can be obtained only with a reduced apparent thermal conductivity of the water-vapor and air mixture.

Acknowledgment

The present work was partially supported by ASI (Agenzia Spaziale Italiana).

Nomenclature

D = water vapor diffusivity in air, [m^2/s]
H_L = latent heat of condensation, [J/kg]
K = thermal conductivity, [W/m K]
l = cubic cell length, [m]
M = molecular mass, [g/mol]
p = pressure, [Pa]
R = gas constant, [J/mol K]
R_V = water vapor gas constant, [J/kg K]
T = temperature, [K]
T_C = temperature, [°C]
V = volume, [m^3]
W = water content, [m^3/m^3]
W_C = adsorbed water content, [m^3/m^3]
W_P = permanent Wilting Point, [m^3/m^3]
W_F = field Capacity, [m^3/m^3]

Greek Symbols

$\beta = l_t/l_s$ = lengths ratio $\delta = W/1-\varepsilon$
$\varepsilon = V_p/V_t$ = porosity
ϕ = air relative humidity
ρ = density, [Kg/m^3]
ξ = mass transfer enhancement factor
γ = lengths ratio
γ_f = lengths ratio

Subscripts

a = air
app = apparent
b = barometric
c = gas phase
d = dry
p = pore
s = solid particle
T = parallel isotherm
t = total
v = water vapor
vs = water vapor at saturation
w = water
wa = adsorbed water
wf = funicular water

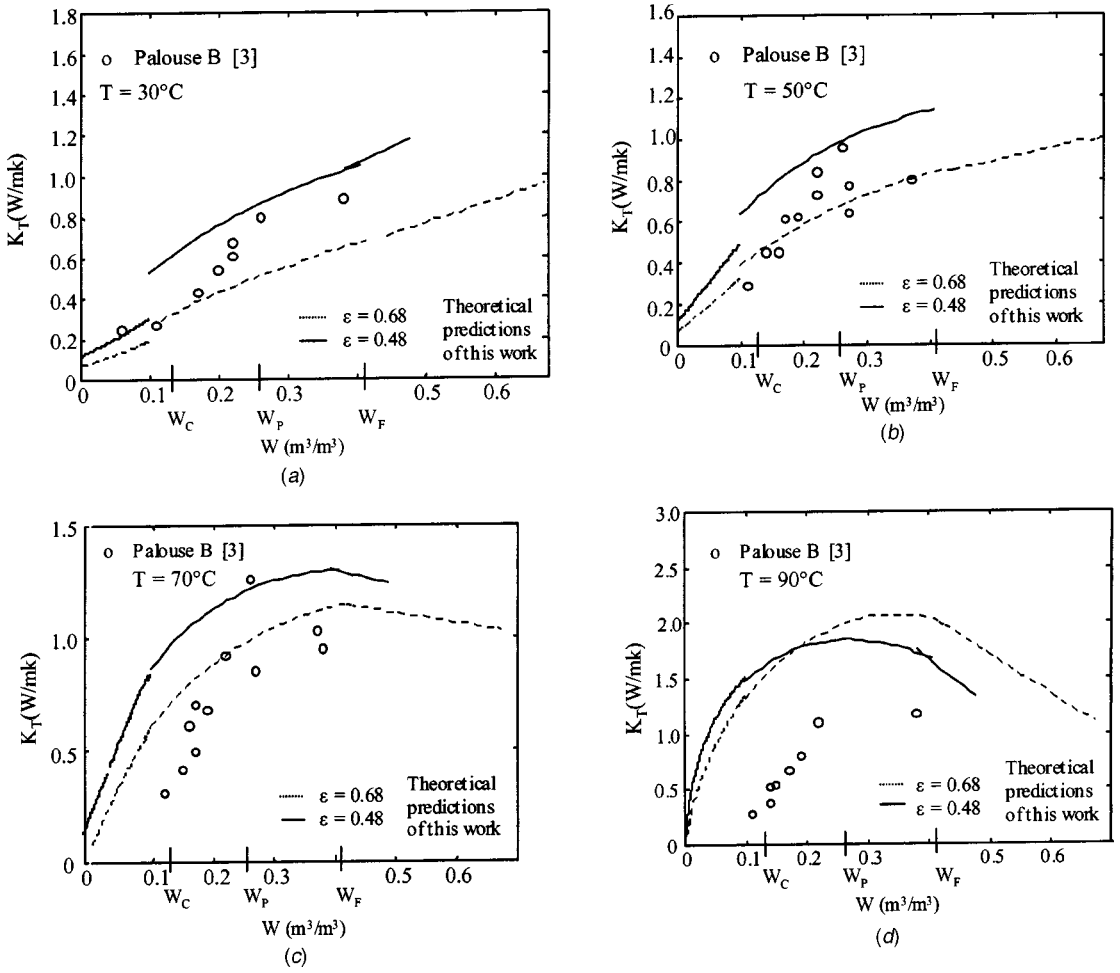

Fig. 6 (*a*) Effective thermal conductivity versus water content in Palouse B [3]; (*b*) effective thermal conductivity versus water content in Palouse B [3]; (*c*) effective thermal conductivity versus water content in Palouse B [3]; and (*d*) effective thermal conductivity versus water content in Palouse B [3].

Appendix A

If the water content is lower than W_C, the effective thermal conductivity is given by, Fig. 1(*b*);

$$\frac{1}{K_T}=\frac{\beta-1-\delta/3}{\beta\cdot K_{\text{app}}}+\frac{\beta\cdot\delta}{3[K_{\text{app}}(\beta^2-1)+K_w)]}+\frac{\beta}{K_s+\frac{2}{3}\cdot\delta\cdot K_w+K_{\text{app}}\left(\beta^2-1-\frac{2}{3}\cdot\delta\right)} \tag{A1}$$

where

$$\delta=\frac{W}{1-\varepsilon}=6\cdot\frac{l_{wa}}{l_s} \tag{A2}$$

The first term of Eq. (*A*1) is the thermal resistance of gas in the section (l_t^2) of length ($l_t-l_s-2l_{wa}$). The second term is the thermal resistance of the materials gas-water in the section (l_t^2) of length ($2l_{wa}$). The third term is the thermal resistance of the materials gas-water-solid in the section (l_t^2) of length (l_s). With reference to Fig. 1(*b*) the three terms can be looked from above to below and also on the plane on the paper.

If $W>W_c$, Fig. 1(*c*) and 1(*d*) the amount of water accumulated among the solid particles is the funicular one, V_{wf}/V_s, according to [20]. In order to simplify the model, V_{wf}/V_s is assumed linearly variable with the real porosity of the medium, between 0.183, for $\varepsilon=0.4764$, and 0.226, for $\varepsilon=0.2595$. The resulting expression is:

$$\frac{V_{wf}}{V_s}=\frac{V_{wf}}{V_p}\cdot(\beta^3-1)=\left[0.183+\frac{0.226-0.183}{0.4764-0.2595}\cdot(0.4764-\varepsilon)\right]\cdot(\beta^3-1) \tag{A3}$$

The following variables are then defined:

$$\gamma=\frac{l_w}{l_s}=\sqrt[3]{\frac{V_w}{V_s}-\frac{V_{wf}}{V_s}+1} \tag{A4}$$

and

$$\gamma_f=\frac{l_{wf}}{l_s}=\sqrt{\frac{V_{wf}/V_s}{3\cdot(\beta-\gamma)}} \tag{A5}$$

In the configuration of Fig. 1(*c*), where $\gamma_f<1$, K_T is given by:

$$\frac{1}{K_T}=\frac{\beta^2-\beta\cdot\gamma}{K_{\text{app}}\cdot(\beta^2-\gamma_f^2)+K_w\cdot\gamma_f^2}+\frac{\beta\cdot\gamma-\beta}{K_{\text{app}}\cdot(\beta^2-\gamma^2)+K_w\cdot\gamma^2}+\frac{\beta-\beta\cdot\gamma_f}{K_{\text{app}}\cdot(\beta^2-\gamma^2)+K_w\cdot(\gamma^2-1)+K_s}+\frac{\beta\cdot\gamma_f}{K_s+K_w\cdot(\gamma^2-1+2\cdot\beta\cdot\gamma_f-2\cdot\gamma\cdot\gamma_f)+A} \tag{A6}$$

where $A=K_{\text{app}}\cdot(\beta^2-\gamma^2-2\cdot\beta\cdot\gamma_f+2\cdot\gamma\cdot\gamma_f)$

The first term of Eq. (*A*6) is the thermal resistance of the materials gas-water in the section (l_t^2) of length (l_t-l_w). The second term is the thermal resistance of the materials gas-water in the section (l_t^2) of length (l_w-l_s). The third term is the thermal resistance of the materials gas-water-solid in the section (l_t^2) of length (l_s-l_{wf}). The fourth term is the thermal resistance of the materials gas-water-solid in the section (l_t^2) of length (l_{wf}). With reference to Fig. 1(*c*) the four sections can be looked from above to below and also on the plane on the paper.

For $\gamma_f>1$, Fig. 1(*d*), K_T has the following expression:

$$\frac{1}{K_T}=\frac{\beta^2-\beta\cdot\gamma}{K_{\text{app}}\cdot(\beta^2-\gamma_f^2)+K_w\cdot\gamma_f^2}+\frac{\beta\cdot\gamma-\beta\cdot\gamma_f}{K_{\text{app}}\cdot(\beta^2-\gamma^2)+K_w\cdot\gamma^2}+\frac{\beta\cdot\gamma_f-\beta}{K_{\text{app}}\cdot(\beta^2-\gamma^2-2\cdot\beta\cdot\gamma_f+2\cdot\gamma\cdot\gamma_f)+K_w\cdot(\gamma^2+2\cdot\beta\cdot\gamma_f-2\cdot\gamma\cdot\gamma_f)}+\frac{\beta}{K_s+K_w\cdot(\gamma^2-1+2\cdot\beta\cdot\gamma_f-2\cdot\gamma\cdot\gamma_f)+K_{\text{app}}\cdot(\beta^2-\gamma^2-2\cdot\beta\cdot\gamma_f+2\cdot\gamma\cdot\gamma_f)} \tag{A7}$$

The first term of Eq. (*A*7) is the thermal resistance of the materials gas-water in the section (l_t^2) of length (l_t-l_w). The second term is the thermal resistance of the materials gas-water in the section (l_t^2) of length (l_w-l_{wf}). The third term is the thermal resistance of the materials gas-water in the section (l_t^2) of length ($l_{wf}-l_s$). The fourth term is the thermal resistance of the materials gas-water-solid in the section (l_t^2) of length (l_s). With reference to Fig. 1(*d*) the four sections can be looked from above to below and also on the plane on the paper.

References

[1] Buckman, H. O., and Brady, N. C., 1975, *The Nature and Properties of Soils* Mac Millan, London.

[2] Ghildyal, B. P., and Tripathi, R. P., 1973, *Soil Physics*, Wiley, London.

[3] Campbell, G. S., Jungbauer, J. D., Bidlake, W. R., and Hungerford, R. D., 1994, ''Predicting the Effect of Temperature on Soil Thermal Conductivity,'' Soil Sci., **158**(5), (pp. 307–313).

[4] de Vries, D. A., 1963, *Thermal Properties of Soils; Physics of Plant Environment*, W. R. Van Wijk, ed., John Wiley and Sons, NY, pp. 210–235.

[5] Sepaskhah, A. R., and Boersma, L., 1979, ''Thermal Conductivity of Soils as a Function of Temperature and Water Content,'' Soil Sci. Soc. Am. J., **43**, pp. 439–444.

[6] Hopmans, J. W., and Dane, J. H., 1986, ''Thermal Conductivity of Porous Media as a Function of Water Content, Temperature and Density,'' Soil Sci., **142**(4), pp. 187–195.

[7] Hiraiwa, Y., and Kasubuchi, T., 2000, ''Temperature Dependence of Thermal Conductivity of Soils Over a Wide Range of Temperature (5–75°C),'' European Journal of Soil Science, **51**, pp. 211–218.

[8] Tarnawski, V. R., Gori, F., Wagner, B., and Buchan, G. D., 2000, ''Modeling Approaches to Predicting Thermal Conductivity of Soils at High Temperatures,'' Int. J. Eng. Res., **24**, pp. 403–423.

[9] Tarnawski, V. R., Leong, W. H., and Bristow, K. L., 2000, ''Developing a Temperature Dependent Kersten Function for Soil Thermal Conductivity,'' Int. J. Eng. Res., **24**, pp. 1335–1350.

[10] Gori, F., 1983, ''A Theoretical Model for Predicting the Effective Thermal Conductivity of Unsaturated Frozen Soils,'' *Proc. of Fourth Int. Conf. on Permafrost*, Fairbanks, AK, pp. 363–368.

[11] Gori, F., 1986, ''On the Theoretical Prediction of the Effective Thermal Conductivity of Bricks'' Proc. of Eight Int. Heat Transfer Conference, San Francisco, II, pp. 627–632.

[12] Hu, Xue-Jiao, Du, Jian-Hua, Lei, Shu-Ye, and Wang, Bu-Xuan, 2001, ''A Model for the Thermal Conductivity of Unconsolidated Porous Media Based on Capillary Pressure-Saturation Relation,'' Int. J. Heat Mass Transf., **44**, pp. 247–251.

[13] Hsu, C. T., Cheng, P., and Wong, K. W., 1995, ''A Lumped-Parameter Model for Stagnant Thermal Conductivity of Spatially Periodic Porous Media,'' ASME J. Heat Transfer, **117**, pp. 264–269.

[14] Fu, X., Viskanta, R., and Gore, J. P., 1998, ''Prediction of Effective Thermal Conductivity of Cellular Ceramics,'' Int. Comm. of Heat and Mass Transfer, **25**(2), pp. 151–160.

[15] Slavin, A. J., Londry, F. A., and Harrison, J., 2000, ''A New Model for the Effective Thermal Conductivity of Packed Beds of Solid Spheroids: Alumina in Helium Between 100 and 500°C,'' Int. J. Heat Mass Transf., **43**, pp. 2059–2073.

[16] Gori, F., Marino, C., and Pietrafesa, M., 2001, ''Experimental Measurements and Theoretical Predictions of the Thermal Conductivity of Two Phases Glass Beads,'' Int. Comm. Heat Mass Transfer, **28**, pp. 1091–1102.

[17] Tarnawski, V. R., and Leong, W. H., 2000, ''Thermal Conductivity of Soils at Very Low Moisture Content and Moderate Temperatures,'' Transport in Porous Media, **1446**, pp. 1–11.

[18] Tarnawski, V. R., and Gori, F., 2002, ''Enhancement of the Cubic Cell Soil Thermal Conductivity Model,'' Int. J. Eng. Res., **26**, pp. 143–157.

[19] Ho, C. K., and Webb, S. W., 1998, ''Review of Porous Media Enhanced Vapor-Phase Diffusion Mechanisms, Models, and Data—Does Enhanced Vapor-Phase Diffusion Exist?,'' Journal of Porous Media, **1**(1), pp. 71–92.

[20] Luikov, A. V., 1966, *Heat and Mass Transfer in Capillary-Porous Bodies*, Pergamon Press.